Serrano-Sillero, J., Moreno, M. N. & Morales, A. (2019). HVDC grids with heterogeneous configuration stations under DC asymmetrical operation. *International Journal of Electrical Power & Energy Systems, 113*, 449–460.

DOI: 10.1016/j.ijepes.2019.05.053

HVDC GRIDS WITH HETEROGENEOUS CONFIGURATION STATIONS UNDER DC ASYMMETRICAL OPERATION

Jesús Serrano-Sillero[a], M. Ángeles Moreno[a], Ana Morales[b]

([a] Universidad Carlos III de Madrid, [b] DIgSILENT Ibérica S.L.)

ABSTRACT

As a response to the future challenges that power systems will have to face, a gradual growth of present High Voltage Direct Current (HVDC) links is expected, leading to an HVDC supergrid integrating different configurations of HVDC stations. Such stations may suffer contingencies affecting just one pole (asymmetrical contingencies). The effects of these contingencies on an HVDC grid are very dependent on the configuration of the HVDC stations and their earthing system. Furthermore, when symmetrical monopolar stations exist in the DC grid, asymmetrical contingencies will also affect its healthy pole. For that reason, this paper focuses on the influence of the earthing system resistance of symmetrical monopolar stations on the performance of a heterogeneous HVDC grid during asymmetrical operation. The impact on the protection system is also investigated. The analysis concludes that an inappropriate earthing resistance magnitude may lead to a poor performance of heterogenous HVDC grids during asymmetrical operation. In addition, the study also indicates that the decisive factors for the selection of the grounding impedance of a symmetrical monopolar station are the asymmetrical operation of the whole grid and its contribution to pole-to-ground fault currents.

Keywords: DC asymmetrical operation, MMC-VSC converters, earthing system, DC faults, contingency.

1. INTRODUCTION

In recent years, there has been an increasing interest in the development of High Voltage Direct Current (HVDC) transmission systems due to two main challenging factors concerning grid operation: the expected rise in electricity consumption in the future, and the growing trend towards a major integration of renewable energies in the energy mix.

In this sense, the HVDC transmission technology is seen as a full solution, specifically the Voltage Source Converter (VSC) technology [1]–[5]. This prevailing view of the VSC-HVDC technology is mainly based on the advantages offered by the Modular Multilevel Converter (MMC) topology [6]: greater transmission capacity than conventional AC lines, extra controllability, inherent ability to interconnect asynchronous systems, or possibility of connecting weak AC systems.

The trend is clear. Not only the technology is extensively deployed in many countries (i.e. France - Spain [7], China [8], [9], North Sea [10]), but also the number of planned VSC-HVDC projects is increasing (Germany [11], USA [12], Germany - Norway [13]).

This future expansion of HVDC links in the world will lead progressively into meshed HVDC grids. Previous studies have reported on the advantages of using a meshed HVDC overlay grid interconnecting the renewable generation in Europe. However, many questions need to be solved effectively before such a grid becomes reality [2], [3], [14]. The bipolar configuration is the most popular, as it offers redundancy to the system and makes it N-1 secure. Nevertheless, different configurations will coexist, forming a heterogeneous meshed HVDC grid.

The future existence of such a grid requires a complete understanding of its behaviour under different circumstances. Many studies have focused on the analysis of HVDC grids with either bipolar [15]–[17] or monopolar [18]–[20] configurations. Hybrid MMC-HVDC configurations based on full-bridge and half-bridge submodules with independent pole control have also been addressed [21]. In the same way, the focal point for most researchers has been the study of the system under balanced operation [22]–[24] or AC unbalanced operation [25]–[33]. An optimisation of the grounding resistor of Luxi back-back project considering DC voltage asymmetries was also addressed in [34]. However, little attention has been paid to the study of an HVDC system integrating different HVDC station configurations under asymmetrical DC operation. This asymmetrical operation, which appears after a contingency affecting a single pole, directly involves the earthing system of the stations. In addition, when symmetrical monopolar stations are involved, a perturbation in one pole is transmitted to the

healthy one, since a single converter controls both poles of the grid. Therefore, in an attempt to take into account all these aspects not considered before, this paper deals with the influence of the earthing resistance of symmetrical monopolar stations on the performance of a heterogeneous meshed DC grid during asymmetrical operation. Different scenarios are analysed to cover the possible control strategies of DC grids and thus, point out the problems that may arise. Furthermore, the impact of the grounding system on the protection system is also addressed.

The paper is organized as follows. Section 2 presents an overview of configurations and earthing options in HVDC links. Section 3 develops the converter equations and delves into the variables influencing the asymmetrical operation. Section 4 assesses selected case studies and scenarios. Finally, the conclusions obtained are gathered in Section 5.

2. HVDC CONVERTER STATION CONFIGURATION AND EARTHING SYSTEM

Fig. 1 shows a representation of three converter station configurations [24]. The symbol E refers to the most frequent locations for the earthing system. The dashed line represents the metallic return.

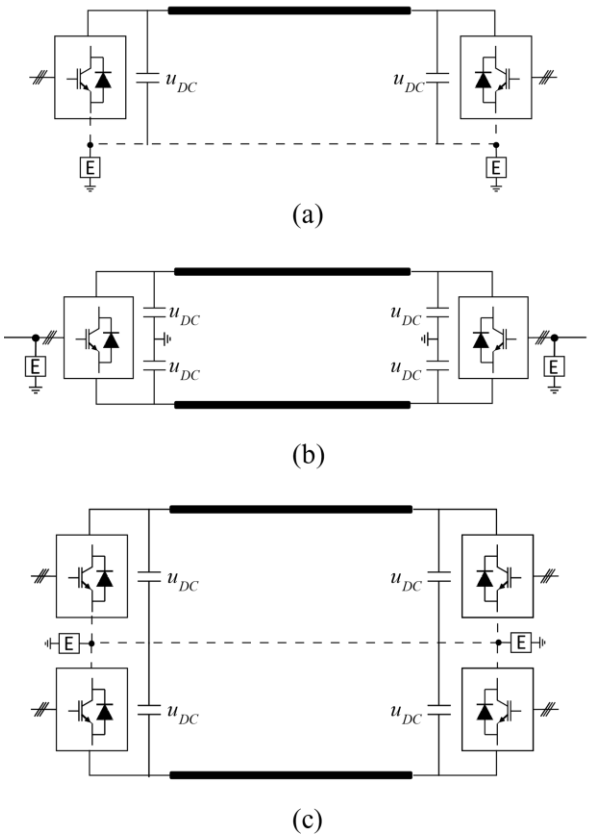

Fig. 1. HVDC converter station configurations: (a) asymmetrical monopole; (b) symmetrical monopole; (c) bipole.

The way an HVDC station is grounded can be classified according to the grounding point (AC side vs DC side), according to the magnitude of the impedance (low or high) or the type of impedance (resistive, inductive, capacitive, or a combination) [24]. A low impedance leads to the appearance of high short-circuit currents during pole to ground faults, whereas a high impedance offers a high voltage stress in the station equipment [22], [23]. The nature of the impedance determines the dynamic behaviour: an inductive impedance limits the rising rate of the fault current and increases the transient overvoltage during a fault, simultaneously; a capacitive impedance limits the rising rate of the voltage while provokes a higher transient fault current; a resistive impedance reduces the steady-state earth current, increases the steady-state DC voltage and damps current or voltage oscillations.

Reference [24] presents alternatives to locate the earthing point in asymmetrical monopolar and bipolar MMC-HVDC stations, although the usual locations are shown in Fig. 1 [23], [35]. The

preferred choice in MMC-HVDC symmetrical monopolar stations is to ground the AC side [18] against the option of high DC resistances to connect both poles to earth at the DC side.

The most frequent AC side grounding methods are shown in Fig. 2. Their purpose is to provide a path for zero-sequence currents. They use typically a Yd transformer with additional grounding equipment such as a star point reactor, a zig-zag grounding transformer or a Yyd transformer with earthing impedance [20]. Additional information about these AC side grounding methods can be consulted in [36]. The zig-zag transformer is more specifically addressed in [18].

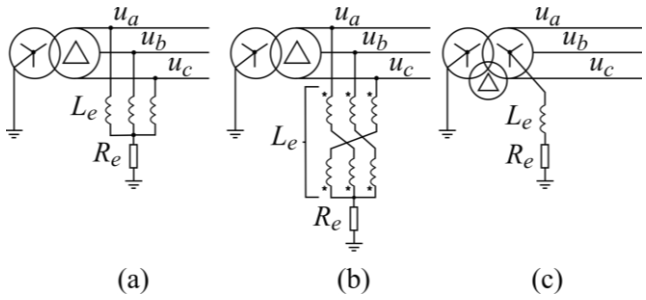

Fig. 2. AC side grounding systems: (a) star point reactor; (b) zig-zag transformer; (c) Yyd transformer with an earthing impedance.

2.1. ASYMMETRICAL MONOPOLE CONFIGURATION

The asymmetrical monopole configuration in Fig. 1 (a) requires only one fully insulated high voltage conductor since the earthed pole uses a metallic conductor or the ground itself as a return path.

In an MTDC system consisting entirely of asymmetrical monopolar stations, at least one of the stations needs to be grounded through a very low resistance electrode [24]. Alternatively, a reactance can be connected in series with the resistance to limit the rising rate of the current in case of faults. The rest of stations in the MTDC system can be connected either to that electrode through a metallic return or they can have their own grounding electrode. It is also recommendable to set more than one grounding point in a large system, in order to keep the voltage in the metallic return low enough. Additionally, the AC side must be isolated from earth in order to prevent a zero-frequency current component flowing through the AC grounding point.

2.2. SYMMETRICAL MONOPOLE CONFIGURATION

The symmetrical monopole configuration shown in Fig. 1 (b) needs a fully insulated high voltage conductor per pole, increasing the cost per installed MW but avoiding issues related to ground currents [23]. In this case, the pole-to-pole DC voltage is the rated DC voltage; each pole has opposite polarity and half rated DC voltage. The type of grounding system determines the system behaviour during pole to ground faults [23], [24].

Any of the options shown in Fig. 2 is valid for the AC side grounding configuration [15]. In the case of the star point reactor, the reactance needs to be high enough to limit reactive power consumption and losses [18]. The zig-zag transformer offers advantages with respect to the star point reactor [18]. It limits the zero-sequence current depending on the magnitude of the earth resistance, like in the star point reactor, but it provides a high impedance path for both positive and negative sequence currents at the same time, avoiding the reactive power consumption during normal operation. Lower reactance values than those used for the star-point reactor can be used. The Yyd transformer with a grounding impedance uses the neutral point of the wye winding of the transformer to ground the system through an impedance, without constraints regarding the magnitude of the resistance or the reactance.

2.3. BIPOLAR CONFIGURATION

The bipolar configuration shown in Fig. 1 (c) can be viewed as two asymmetrical monopoles connected to each other by sharing the pole connected to ground. Although the cost increases, the redundancy justifies the higher investment. Both poles are subjected to the converter nominal DC voltage, with opposite polarity [23]. In a bipolar system, a metallic conductor or the ground can be used as return path like in the asymmetrical monopolar configuration. In this way, each pole can continue working like an asymmetrical monopole in case the other pole is disconnected [24]. Regarding the behaviour during faults, it depends entirely on the type of grounding system [22], [23]. The bipolar configuration can be isolated or grounded at the DC side. In case of zero grounding

impedance, or when the return path is the earth itself, this system behaves like the asymmetrical monopole during pole-to-ground faults. When the system is isolated or grounded through a high impedance, the neutral conductor will have to be insulated, increasing the costs. Regarding the grounding of the AC side, the same concerns that have been highlighted for the asymmetrical monopolar stations [24] can be considered for the bipolar stations.

3. ASYMMETRY IN DC GRIDS

Contingencies in heterogeneous meshed HVDC grids can eventually result in a DC grid asymmetry, which occurs when the positive and negative poles of an HVDC station do not carry the same current and/or do not have the same voltage (absolute value). The DC asymmetrical operation manifests itself as a zero-sequence component in the voltage and/or current on the converter AC-side.

In Fig. 3, phase-*j* of a three-phase MMC converter is represented, where i_{AC}^{j} is the AC current flowing into the converter, u_{AC}^{j} is the phase-*j* AC voltage, i_{DC}^{+} and i_{DC}^{-} are the positive and negative DC-pole currents, and u_{DC}^{+} and u_{DC}^{-} are the positive and negative DC-pole voltages respectively.

According to the references given in Fig. 3, the following equations can be derived:

$$\begin{cases} i_u^j = i_{diff}^j + \dfrac{i_{AC}^j}{2} \\ i_l^j = i_{diff}^j - \dfrac{i_{AC}^j}{2} \end{cases} \qquad (1)$$

where i_u^j and i_l^j are the upper and lower arm currents in phase-*j*, respectively, and i_{diff}^j is a current circulating through the phase-*j* leg and the DC link. Then:

$$i_{AC}^j = i_u^j - i_l^j \qquad (2)$$

$$i_{diff}^j = \frac{i_u^j + i_l^j}{2} \qquad (3)$$

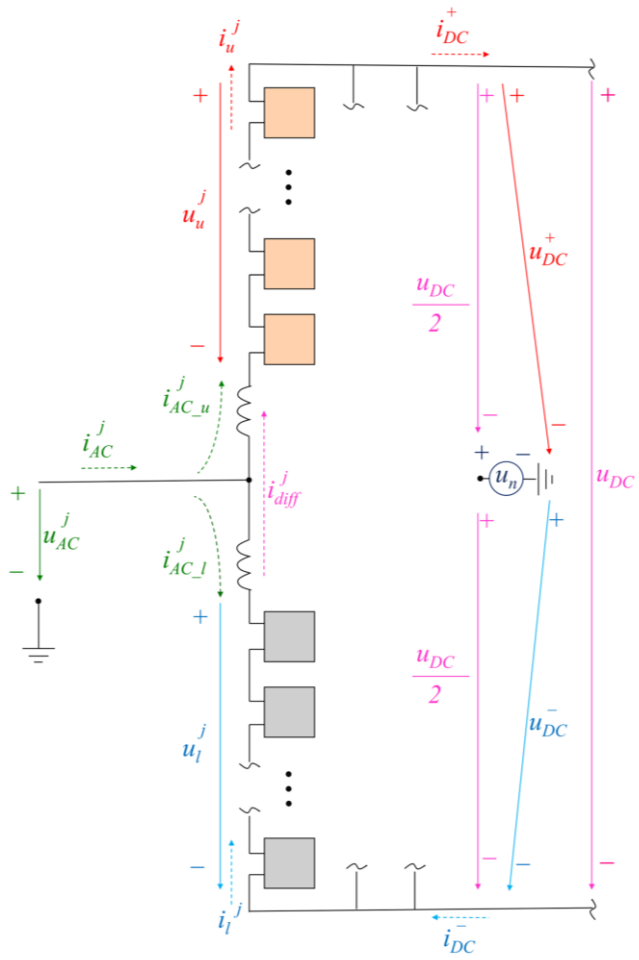

Fig. 3. Schematic diagram of one phase of an MMC-HVDC converter. Voltages are represented with solid arrows and currents with dashed arrows.

Considering the three phases, DC currents flowing through the positive and negative poles are calculated as follows:

$$i_{DC}^{+} = \sum_{j=1}^{3} i_u^j = \sum_{j=1}^{3} i_{diff}^j + \frac{1}{2}\sum_{j=1}^{3} i_{AC}^j \qquad (4)$$

$$i_{DC}^{-} = \sum_{j=1}^{3} i_l^j = \sum_{j=1}^{3} i_{diff}^j - \frac{1}{2}\sum_{j=1}^{3} i_{AC}^j \qquad (5)$$

Summing and subtracting (4) and (5):

$$i_{DC}^{+} + i_{DC}^{-} = 2\sum_{j=1}^{3} i_{diff}^j \qquad (6)$$

$$i_{DC}^{+} - i_{DC}^{-} = \sum_{j=1}^{3} i_{AC}^{j} \qquad (7)$$

From the previous equations, it can be deduced that:

- When no zero-sequence AC current exists, positive and negative DC-pole currents are equal:

$$i_{DC}^{+} = i_{DC}^{-} = i_{DC} = \sum_{j=1}^{3} i_{diff}^{j} \qquad (8)$$

- When positive and negative DC-pole currents differ, then a zero-sequence current appears at the AC side:

$$i_{DC}^{+} - i_{DC}^{-} = 3i_{AC_0} \qquad (9)$$

Applying Kirchhoff's voltage law to the upper and lower converter arms of the phase-*j* in Fig. 3 yields:

$$u_u^j = u_{DC}^{+} - u_{AC}^{j} + L_{arm}\frac{di_u^j}{dt} \qquad (10)$$

$$u_l^j = u_{DC}^{-} + u_{AC}^{j} + L_{arm}\frac{di_l^j}{dt} \qquad (11)$$

In Fig. 3, a DC offset voltage (u_n) is included in the fictitious DC-side neutral point to account for asymmetries in the positive and negative DC-pole voltages:

$$\begin{cases} u_{DC}^{+} = \dfrac{u_{DC}}{2} + u_n \\ u_{DC}^{-} = \dfrac{u_{DC}}{2} - u_n \end{cases} \qquad (12)$$

Accordingly, the pole-to-pole DC voltage and the DC offset voltage are given by:

$$u_{DC} = u_{DC}^{+} + u_{DC}^{-} \qquad (13)$$

$$u_n = \frac{u_{DC}^{+} - u_{DC}^{-}}{2} \qquad (14)$$

Subtracting (10) from (11) yields:

$$u_l^j - u_u^j = -2u_n + 2u_{AC}^j - L_{arm}\frac{di_{AC}^j}{dt} \qquad (15)$$

A new variable can be introduced, which can be regarded as a virtual potential [19], [37]:

$$e^j = \frac{u_l^j - u_u^j}{2} \qquad (16)$$

Then, Eq. (15) can be written as:

$$e^j = u_{AC}^j - \frac{L_{arm}}{2}\frac{di_{AC}^j}{dt} - u_n \qquad (17)$$

From Eq. (17), and considering the three phases, the zero-sequence equation is derived:

$$e_0 = u_{AC_0} - \frac{L_{arm}}{2}\frac{di_{AC_0}}{dt} - u_n \qquad (18)$$

From the previous equation, it can be deduced that:

- When the positive and negative DC-pole voltages are equal, the neutral point voltage is zero, and there is no zero-sequence AC voltage.

$$u_{DC}^+ = u_{DC}^- = \frac{u_{DC}}{2} \qquad (19)$$

- When the positive and negative DC-pole voltages differ, a zero-sequence AC voltage appears in the system:

$$u_{AC_0} = e_0 + \frac{L_{arm}}{2}\frac{di_{AC_0}}{dt} + u_n \qquad (20)$$

If the converter is grounded on its AC side, Eq. (20) can be rewritten by replacing u_{AC_0} with the voltage drop through the equivalent grounding impedance:

$$u_n = -e_0 - \left(\frac{L_{arm}}{2} + L_e\right)\frac{di_{AC_0}}{dt} - R_e \cdot i_{AC_0} \qquad (21)$$

Therefore, the DC asymmetric operation is related to the zero–sequence quantities on the AC side of the converter.

Under DC asymmetric operation, the power asymmetry (PA) between poles is defined by:

$$PA = P_{DC}^{+} - P_{DC}^{-} = u_{DC}^{+} \cdot i_{DC}^{+} - u_{DC}^{-} \cdot i_{DC}^{-} \qquad (22)$$

Considering Eqs. (9) and (12), the power asymmetry can be expressed as follows:

$$PA = u_n \left(i_{DC}^{+} + i_{DC}^{-} \right) + 3 i_{AC_0} \frac{u_{DC}}{2} \qquad (23)$$

Equation (23) reveals the main variables that affect the DC power asymmetry, making easier the study of these quantities from the point of view of DC systems. In (23), the pole-to-pole DC voltage is unaffected by the DC offset voltage (see Eq. (13)) and, therefore, also by the zero-sequence. On the other hand, the sum of the positive and negative DC-pole currents is unaffected by the zero-sequence (see Eq.(6)). Thus, it can be said that the first term in Eq. (23) represents the power asymmetry due to voltage asymmetry, whereas the second term stands for the power asymmetry caused by a current asymmetry. The second term only appears in symmetrical monopolar stations since they can be earthed on their AC side.

Therefore, from equations developed in this section, in case of asymmetrical operation in an HVDC system due to a contingency, the impact on the quantities of the system can be assessed based on:

- The magnitude of the power asymmetry. As expressed by Eq. (22), a contingency or fault affecting both DC poles will not produce any asymmetry. If it affects just one of them, the higher the power missing, the higher the asymmetry.
- The earthing system and topology of the HVDC station. When an asymmetry in DC-pole currents and/or voltages occurs, a zero-sequence voltage and/or current appears on the AC side of the converter. The contribution of all these quantities to the power asymmetry depends on the topology and the earthing system, as expressed by Eq. (23).

However, additional aspects will have an influence on the dynamic behaviour of the entire system during asymmetrical operation. The earthing impedance of symmetrical monopolar stations transfers the perturbation from the affected pole of the grid to the healthy one in the form of DC current and/or

voltage asymmetry. As a result, positive and negative pole converters will react to an asymmetrical perturbation according to Eqs. (4), (5) and (12) in an opposite direction. Therefore, the control strategy of the HVDC grid and the stations involved are also a key aspect during asymmetrical operation. A case study approach is used in the next section to obtain a general overview of the problems that may arise due to the asymmetrical operation of the grid under different possible circumstances. This comprehensive analysis makes possible to obtain guidelines and recommendations to select an appropriate grounding impedance for each situation.

4. STUDY CASES

The behaviour of an HVDC system during an asymmetrical operation is analysed in this paper through EMT simulations performed in DIgSILENT PowerFactory. Several cases are examined to study the impact of the earthing impedance of symmetrical monopolar stations on the HVDC system under different circumstances. Cases 1-4 analyse the influence of the earthing resistance of symmetrical monopolar stations on the response of an HVDC system during asymmetrical operation considering the most usual control strategies of HVDC grids. Cases 5-6 evaluate the impact of the earthing impedance of symmetrical monopolar stations on the protection system of the HVDC grid. The purpose of this analysis is to provide guidelines to choose a suitable earthing impedance for symmetrical monopolar stations in heterogeneous HVDC grids.

The heterogeneous three-terminal HVDC grid used in this demonstration is depicted in Fig. 4. Two bipolar stations (Cb-A, Cb-B) and one symmetrical monopole station (Cm-C) are interconnected. All converters are considered to be MMC-VSC type. The asymmetrical operation is obtained with the outage of one of the converters of a bipolar station. The main parameters are gathered in Table 1. The converter controllers are extracted from [38].

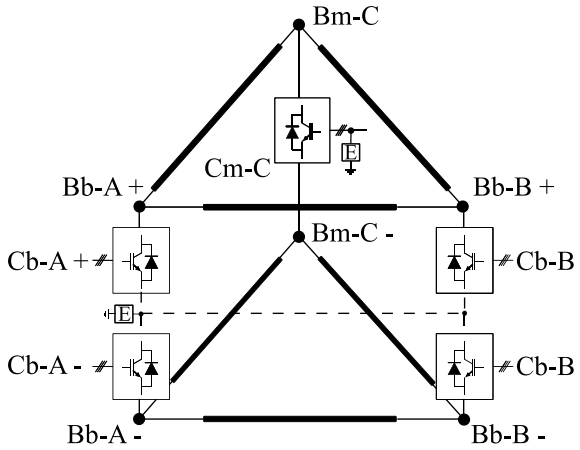

Fig. 4. Three-terminal meshed heterogeneous HVDC system.

Table 1: Parameters of the system.

AC grid system voltage	220 kV RMS
Nominal frequency	50 Hz
DC grid system voltage	+/-350 kV
Rated active power of converters	800 MW
Number of SMs per arm	400
SM capacitor	10 mF
Arm inductor	28 mH
Line length	200 km
Line parameters (R, L, G, C) (For 0.001 Hz)	0.011 Ω/km, 0.9356 mH/km, 0μS/km, 0.0123 μF/km

Regarding the grounding system, the dashed line in Fig. 4 represents the metallic return; in-squared "E" indicates the grounding points. Cb-A bipolar station is rigidly earthed and none of the systems shown in Fig. 2 is specifically used for the symmetrical monopolar station because the purpose is to obtain general conclusions without focusing on any predefined grounding topology. In fact, the three grounding systems shown in Fig. 2 for symmetrical monopolar stations behave like a reactance in series with a resistance from the zero-sequence point of view. Thus, in each case, three different values for the grounding resistance (R_e) in the AC side of the symmetrical monopolar HVDC station Cm-C are considered: a) 0 p.u., b) 0.5 p.u., c) ∞ p.u.

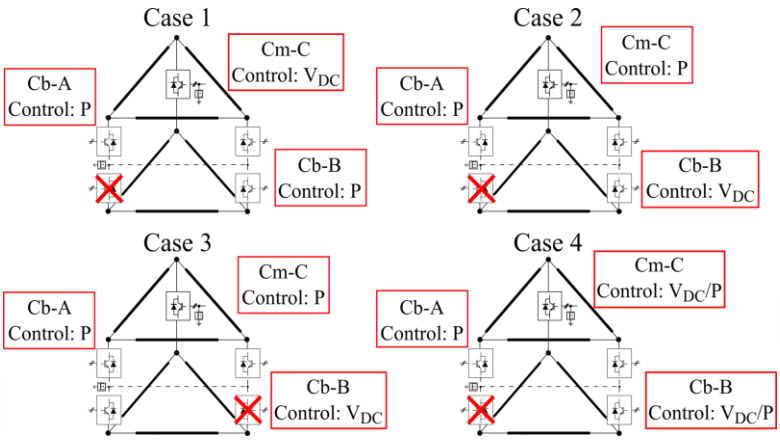

Fig. 5. Negative pole outage in four different cases for asymmetrical operation analysis.

Fig. 5 shows a brief overview of the selected study cases 1-4, indicating the negative pole under outage (following a contingency) and the control mode in each HVDC station.

The dynamic behaviour of the grid in each case is analysed through the evolution of DC voltages and currents and zero-sequence quantities on the AC side of Cm-C. Moreover, DC and AC active power flow in the HVDC stations are examined. Power is positive when flowing from the AC side to the DC side, according to the references in Fig. 3.

4.1. CASE 1

In this first case, the monopolar converter is assuming the voltage control of the DC grid. Both bipolar stations are operating in constant active power transfer mode. The loss of the negative pole at the Cb-A station is analysed. Current and voltage responses in Cm-C converter are shown in Fig. 6. In addition, Fig. 7 shows the AC and DC active power flow in the three stations.

When the converter is grounded, the change in DC voltage results in the actuation of the Cm-C DC voltage controller to keep the pole-to-pole DC voltage at the setpoint value, but the system may become unstable in case of null grounding resistance, as the red curves show in Fig. 6. This is due to two opposite effects: a) the Cm-C DC-pole voltages cannot change from their initial value to the new steady state since there is no zero-sequence voltage and the pole-to-pole DC voltage is fixed by the controller; b) the zero-sequence current injection resulting from the asymmetry tends to change the DC-pole voltages in the opposite direction, also involving the power controller of the other HVDC

stations. Additionally, this instability is transferred as undamped oscillations of active power to the AC-side of the Cm-C HVDC station, as seen in the three upper graphs in Fig. 7. By contrast, if the value of the earthing resistance increases, the power oscillation damping also increases, and the system is stable after the disturbance.

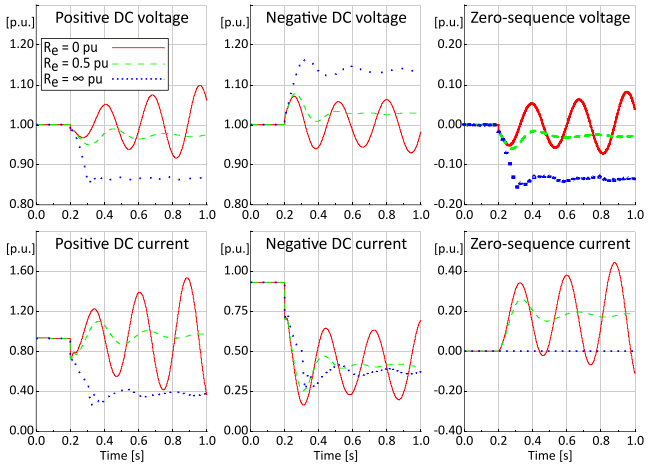

Fig. 6. Case 1 – Cm-C currents (i_{DC}^{+}, i_{DC}^{-} and i_{AC_0}) and voltages (u_{DC}^{+}, u_{DC}^{-} and u_{AC_0}) under different values of the Cm-C earthing resistance.

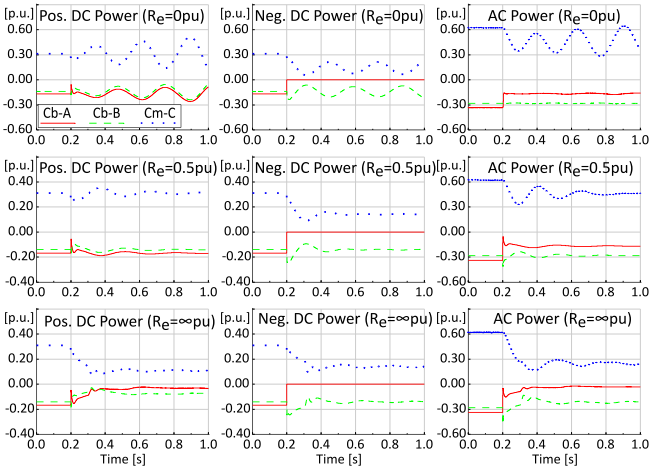

Fig. 7. Case 1 - DC and AC active power flows in the three HVDC stations under different values of the Cm-C earthing resistance.

When the system is isolated from ground ($R_e = \infty$), the DC voltage variation after the contingency results in a zero-sequence voltage on the AC side of the Cm-C HVDC station. This voltage leads the system to a new steady-state at a higher voltage level at one pole (negative pole) and a lower voltage

level at the other pole (positive pole) (Fig. 6). The increase in the pole voltage will negatively affect the insulation level. The voltage drop of the other pole will saturate the converter and reduce its transmission capacity, resulting in an imbalance of power on the AC side (Fig. 7). This impact can be reduced by decreasing the earthing resistance value of Cm-C station.

4.2. CASE 2

In this case, the Cb-B bipolar station is responsible for the DC voltage control of the system and the other stations work in power control mode (see Fig. 5). Under these control conditions, the outage of the negative pole at the Cb-A station is analysed.

Fig. 8 shows the voltage and current response of Cm-C station whereas the DC and AC power flow in each HVDC station are plotted in Fig. 9. In this case, only the negative pole in Cb-B HVDC station changes its active power contribution after the contingency.

Looking at Fig. 8, the system becomes unstable when the grounding resistance is zero, as in the previous case. From Eq. (21), it is clear that as long as the positive and negative DC voltages differ from one another, the derivative of the zero-sequence current on the AC side is not null when the resistive part of the grounding impedance is zero. Therefore, the zero-sequence current increases continuously. The Cm-C HVDC station should be disconnected in this case, since the uncontrolled rise in zero-sequence current results in an overcurrent in the three upper arms. Increasing the value of the earthing resistance improves the system stability.

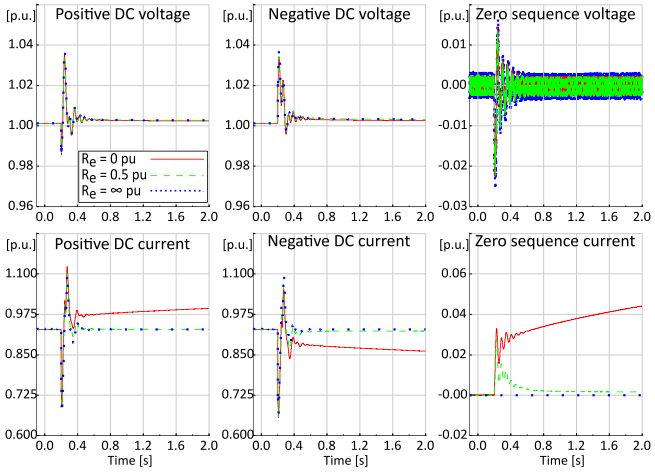

Fig. 8. Case 2 – Cm-C currents (i_{DC}^{+}, i_{DC}^{-} and i_{AC_0}) and voltages (u_{DC}^{+}, u_{DC}^{-} and u_{AC_0}) under different values of the Cm-C earthing resistance.

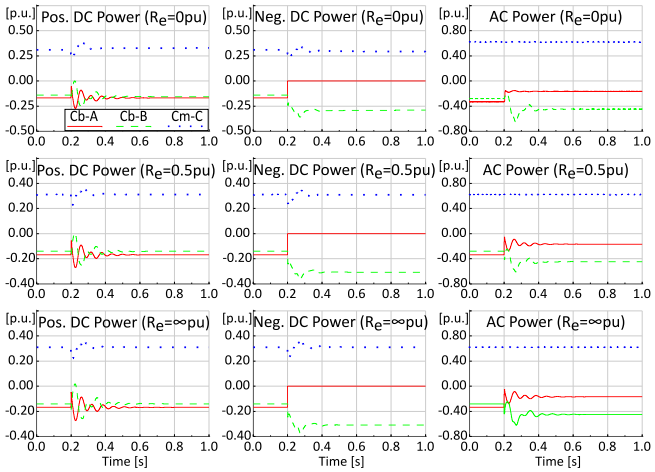

Fig. 9. Case 2 - DC and AC active power flows in the three HVDC stations under different values of the Cm-C earthing resistance.

When the system is isolated from ground, the pole outage causes a transient voltage at the DC-poles, but the system is stable. In addition, the Cb-B DC voltage controller acts and drives voltage to its reference value in the three scenarios under analysis, because each pole of the bipolar station Cb-B can control the positive and negative DC voltage independently. Nevertheless, a small voltage asymmetry always exists in the system due to different losses in both poles of the DC grid. From Fig. 9, it can be inferred that there is no apparent influence of the earthing resistance on the AC power injection.

4.3. CASE 3

The purpose of this case is to show the behaviour of the system when one of the poles of the HVDC station that controls the DC voltage (Cb-B) is disconnected, being the remaining converters in active power control mode. It is worth mentioning that the control strategy of the grid is the same as in the previous case; what changes is the control mode of the converter suffering the outage.

Fig. 10 displays the voltages and currents at the Cm-C HVDC station. Fig. 11 shows the DC and AC active power flow in each station.

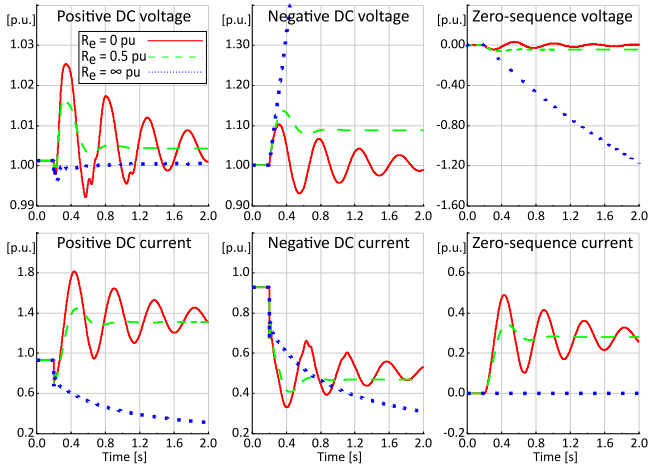

Fig. 10. Case 3 – Cm-C currents (i_{DC}^{+}, i_{DC}^{-} and i_{AC_0}) and voltages (u_{DC}^{+}, u_{DC}^{-} and u_{AC_0}) under different values of the Cm-C earthing resistance.

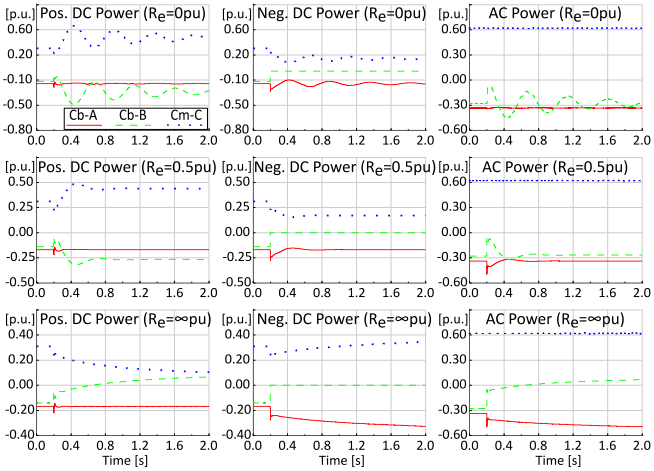

Fig. 11. Case 3 - DC and AC active power flows in the three HVDC stations under different values of the Cm-C earthing resistance.

When the converter Cm-C is grounded, the appearance of the zero-sequence quantities due to the asymmetry transfers the disturbance to the healthy pole and contributes to balance the DC voltage in the affected one. Moreover, the positive Cb-B converter regulates its active power injection in order to keep the positive DC voltage setpoint, stabilizing also the negative pole. Although the system is stable, a resistive earthing value improves the damping of the oscillations on both the DC and the AC side, as observed in Fig. 10 and Fig. 11. However, because of the zero-sequence current, the positive DC current increases and the negative one decreases (see Fig. 10). An increase of the Cm-C earthing resistance will reduce the zero-sequence current and, thus, the overcurrent. However, it will produce a DC overvoltage.

Unlike the previous cases, the system becomes unstable when the Cm-C station is isolated from ground. The DC current imbalance at the negative pole causes an increase in the DC voltage at that pole. The positive DC voltage remains almost constant since the positive pole of the Cb-B converter controls the DC voltage. Since the control logic of the Cm-C converter tries to keep the active power constant, the DC current at both poles must progressively decrease. The negative DC voltage will continue to rise steadily until the currents at the negative pole of the grid reach a new balance. The negative DC voltage reaches about 3.40 p.u. after 2 seconds of simulation, but the scale in Fig. 10 is adjusted to a lower value to improve the visualization and analysis.

Notice that the network control strategy in cases 2 and 3 are the same before the contingency, but results are different. Therefore, the control strategy of the HVDC grid and the grounding impedance of symmetrical monopolar stations are not the only aspects impacting the asymmetrical operation, but also the control mode of the lost converter.

4.4. CASE 4

The outage of a pole in an HVDC station that operates in active power control mode is simulated, with the rest of converter stations in Vdc/P droop control mode. In this case, two different droop gains (K_{DROOP}) have been considered: a) 0.05 p.u. and b) 1 p.u.

Fig. 12 and Fig. 13 show that the system is unstable for any of the values of earthing resistance when K_{DROOP} is 0.05 p.u. This is due to the high level of sensitivity to voltage deviations rather than to the resistance value. Therefore, the contingency leads the system to instability, affecting both DC and AC sides.

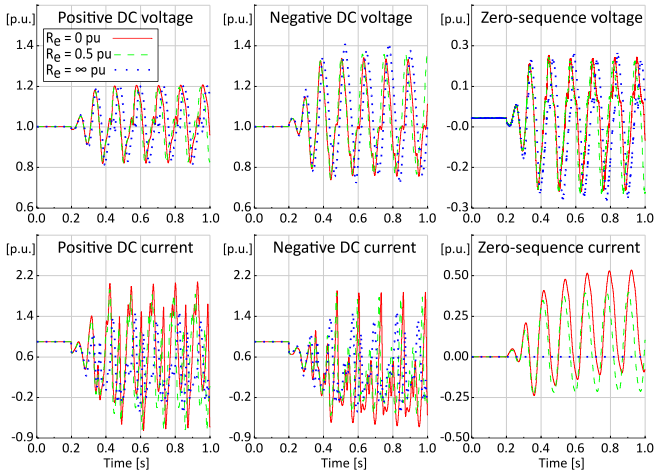

Fig. 12. Case 4, K_{DROOP} = 0.05 p.u. – Cm-C currents (i_{DC}^{+}, i_{DC}^{-} and i_{AC_0}) and voltages (u_{DC}^{+}, u_{DC}^{-} and u_{AC_0}) under different values of the Cm-C earthing resistance.

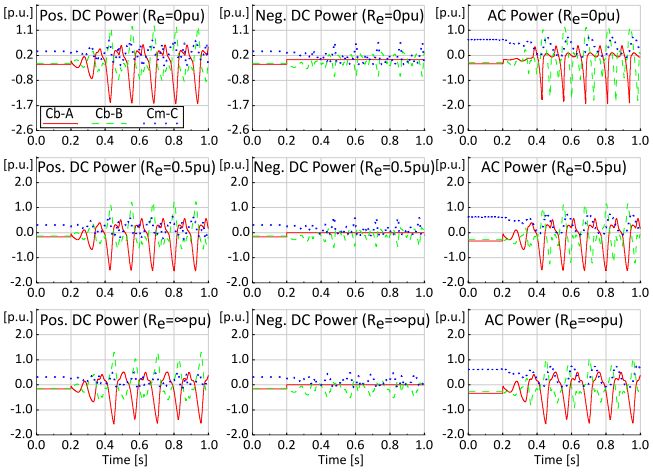

Fig. 13. Case 4, K_{DROOP} = 0.05 p.u. - DC and AC active power flows in the three HVDC stations under different values of the Cm-C earthing resistance.

If K_{DROOP} = 1.00 p.u., the system maintains stability for all the scenarios evaluated, as shown in Fig. 14 and Fig. 15. The fact of using one of the grounding systems or another has a great impact on

overcurrents and voltage deviations produced in the system during the transient, as well as in the new steady state.

The voltage deviation increases with the increase in Cm-C earthing resistance value, while the overcurrent is reduced. The largest voltage deviation appears when the Cm-C station is not grounded, as seen in Fig. 14. This can cause two problems depending on the sign of the deviation: a high voltage level endangers all the equipment; an excessive low voltage can saturate converters and limit their transmission capacity.

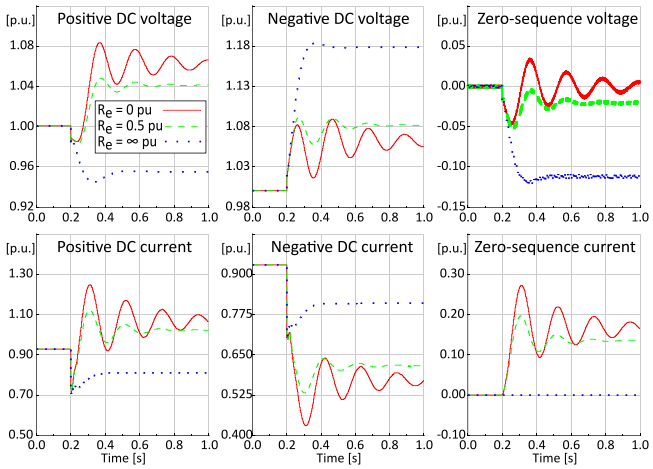

Fig. 14. Case 4, K_{DROOP} = 1.00 p.u. – Cm-C currents (i_{DC}^{+}, i_{DC}^{-} and i_{AC_0}) and voltages (u_{DC}^{+}, u_{DC}^{-} and u_{AC_0}) under different values of the Cm-C earthing resistance.

However, Fig. 14 shows that the highest current appears when the Cm-C station grounds through a zero resistance. Therefore, all equipment is at risk of damage in this scenario, unless the protections act. Therefore, a compensation between the value of the highest current and the magnitude of the voltage deviation is necessary through the selection of an adequate resistance value. As for the AC side, the earthing resistance has no effect on the active power injected (see Fig. 15), unless the converters saturate as result of low DC voltage.

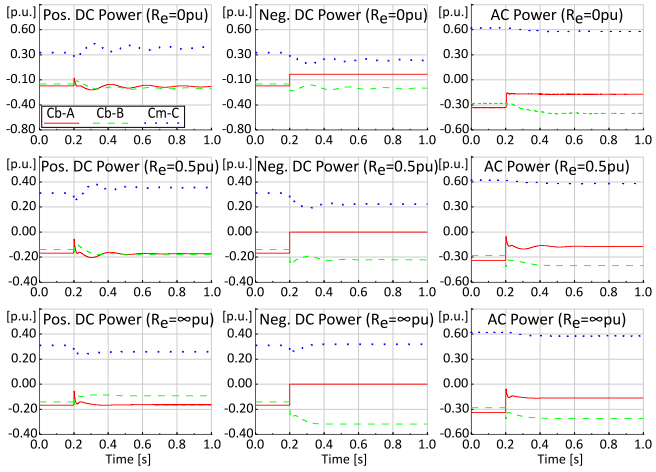

Fig. 15. Case 4, K_{DROOP} = 1.00 p.u. - DC and AC active power flows in the three HVDC stations under different values of the Cm-C earthing resistance.

Table 2 summarizes the critical situations during asymmetrical operation in each study case depending on the grounding resistance value of the symmetrical monopolar station. Although the 0.5 p.u. resistance value offers a good behaviour in most cases, it is worth mentioning that a different resistance value could lead the system to overcurrent, overvoltage, saturation of converters, power oscillation or even unstable situations.

Table 2. Summary of effects produced by the asymmetrical operation in the different cases.

	Earthing Resistance		
Study Cases	**0 p.u.**	**0.5 p.u.**	**∞ p.u.**
Case 1	DC current instability AC power oscillations	-	DC overvoltage Converter saturation
Case 2	DC current instability DC overcurrent	-	-
Case 3	DC overcurrent AC power oscillations	DC overcurrent	DC overvoltage DC voltage instability
Case 4 (K_{DROOP} = 0.05)	General instability	General instability	General instability
Case 4 (K_{DROOP} = 1)	DC overcurrent	-	DC overvoltage Converter saturation

4.5. CASES 5 AND 6

Based on the analysis of cases 1-4, a suitable earthing impedance can be chosen for symmetrical monopolar stations to improve the dynamic response during asymmetrical operations. However, when a new HVDC station is connected to a DC system, the grounding impedance also affects short-circuit currents. That is why the main purpose of these cases is to assess the impact of the Cm-C grounding impedance on the short-circuit currents in the event of a pole-to-ground fault. It is assumed that the neutral point of the two bipolar HVDC stations is connected through a metallic return that is solidly earthed in Cb-A station.

A pole-to-ground fault at the negative pole of the line connecting Cm-C and Cb-A stations has been simulated in two different locations as shown in Fig. 16. In the first case, the fault is close to the Cb-A station, whereas in the second, it is close to Cm-C station. Short-circuit currents flowing through the line to the fault are examined in both cases.

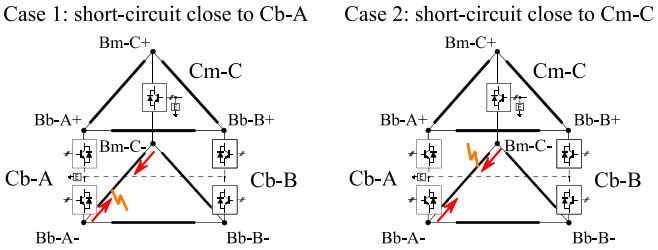

Fig. 16. Short-circuit location in two different cases for asymmetric operation analysis.

Results are depicted in Fig. 17 and Fig. 18. The two upper graphs of each figure compare the currents obtained with a high reactance and three different magnitudes of resistance, while the two lower graphs compare the currents with zero grounding resistance and two different inductance values. The graphs on the left show the currents flowing from terminal Bm-C towards the fault and the graphs on the right show the currents flowing from the terminal Bb-A.

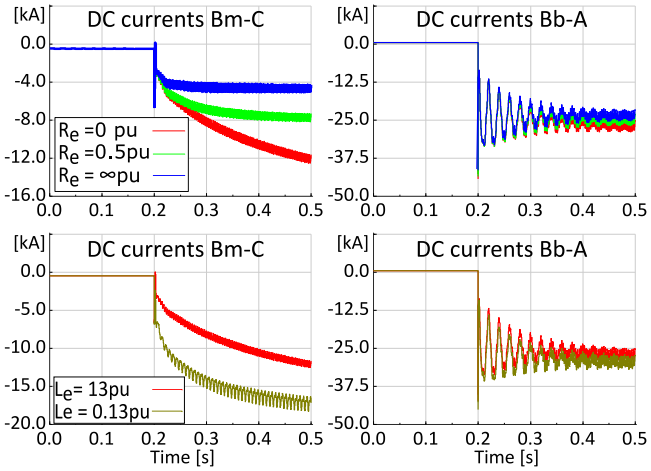

Fig. 17. Case 5 - Short-circuit currents at both ends of the line under different Cm-C earthing systems when the fault is near Cb-A station.

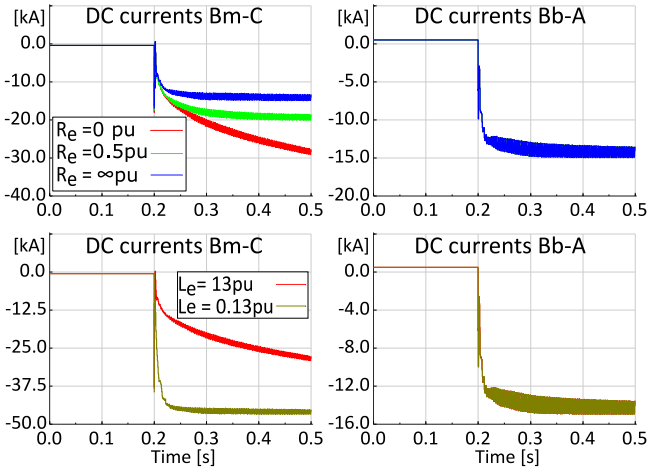

Fig. 18. Case 6 - Short-circuit currents at both ends of the line under different Cm-C earthing systems when the fault is near Cm-C station.

From the analysis of Fig. 17 and Fig. 18, it can be concluded that the grounding impedance significantly influences the short-circuit currents flowing from Bm-C terminal (Cm-C station). The impact is less important on short-circuit currents flowing from Bb-A terminal (Cb-A station), but it is still important as the short-circuit current is growing gradually, achieving a difference of several kA after the first three hundred milliseconds of the fault.

Therefore, the grounding impedance of symmetrical monopolar stations barely modifies the contribution from the rest of converter stations to the short-circuit current during the first moments after the fault. This suggests that the connection of a new symmetrical monopolar station to an HVDC

system with bipolar stations will not affect the existing fast-acting protections in the system. Hence, the dimensioning of the symmetrical monopolar station grounding impedance should be selected considering two criteria: aiming a proper operation of the grid during asymmetrical conditions and the contribution of this station to short-circuit currents.

5. CONCLUSIONS

In this work, the effect of the grounding impedance of symmetrical monopolar stations on heterogeneous meshed HVDC grids is analysed for the first time, as far as the authors know. One of the most significant findings is that the magnitude of the earthing resistance plays a key role in case of asymmetrical operation of the HVDC grid. The results of this study indicate that the magnitude of this resistance should be chosen according to the global control strategy of the HVDC grid and the control mode of the lost converter. Otherwise, inappropriate values can lead to overcurrents, overvoltages, saturation of converters, power oscillations or instability situations. In general, the use of a grounding resistance offers a satisfactory performance in most cases, but specific analyses of the particular cases are recommended.

It is also shown that the grounding impedance of symmetrical monopolar stations barely modifies the short-circuit current contribution from the rest of stations during the first tens of milliseconds after a pole to ground fault. Fast-acting protection systems will clear the short-circuit contribution from the rest of converters before any impact can be observed. This suggests that the criteria to select the grounding impedance of symmetrical monopolar stations should focus on the performance during asymmetrical operations and their current contribution in case of pole to ground faults.

Additionally, this paper highlights the complexity of defining a single methodology to be applied to all HVDC grids, due to their different technology and specific grid planning development. Special attention should be paid when designing and planning HVDC grids with heterogeneous configuration stations to guarantee the viability and reliability even under asymmetrical operation. These findings provide insights for future research on the impact of the design parameters on the system dynamics,

implementation of zero-sequence controls in symmetrical monopolar stations to improve the dynamic response and the development of rules for the design of the grounding impedance under asymmetrical operation.

6. REFERENCES

[1] S. Gordon, "Supergrid to the rescue [electricity supply security]," *Power Eng.*, vol. 20, no. 5, p. 30, 2006.

[2] R. Adapa, "High-wire act: HVdc technology: The state of the art," *IEEE Power Energy Mag.*, vol. 10, no. 6, pp. 18–29, 2012.

[3] D. Van Hertem, M. Ghandhari, and M. Delimar, "Technical limitations towards a SuperGrid - A European prospective," *2010 IEEE Int. Energy Conf. Exhib. EnergyCon 2010*, pp. 302–309, 2010.

[4] M. H. Okba, M. H. Saied, M. Z. Mostafa, and T. M. Abdel- Moneim, "High voltage direct current transmission - A review, part I," in *2012 IEEE Energytech*, 2012, pp. 1–7.

[5] V. Akhmatov *et al.*, "Technical guidelines and prestandardization work for first HVDC Grids," *IEEE Trans. Power Deliv.*, vol. 29, no. 1, pp. 327–335, 2014.

[6] B. Gemmell, J. Dorn, D. Retzmann, and D. Soerangr, "Prospects of multilevel VSC technologies for power transmission," in *2008 IEEE/PES Transmission and Distribution Conference and Exposition*, 2008, pp. 1–16.

[7] P. L. Francos, S. S. Verdugo, H. F. Alvarez, S. Guyomarch, and J. Loncle, "INELFE — Europe's first integrated onshore HVDC interconnection," in *2012 IEEE Power and Energy Society General Meeting*, 2012, pp. 1–8.

[8] X. Li, Z. Yuan, J. Fu, Y. Wang, T. Liu, and Z. Zhu, "Nanao multi-terminal VSC-HVDC project for integrating large-scale wind generation," in *2014 IEEE PES General Meeting | Conference & Exposition*, 2014, pp. 1–5.

[9] Y. Li, H. Xiaoming, J. Zhang, and W. Sun, "China Upgrades Capacity to the Zhoushan Islands,"

Transmission and Distribution World, 2017. [Online]. Available: https://www.tdworld.com/digital-innovations/china-upgrades-capacity-zhoushan-islands. [Accessed: 25-Jan-2019].

[10] Prysmian Group, "Prysmian secures SylWin1 project by TenneT for the cable connection of offshore wind farms in the North Sea to the German power grid," *Press Releases*, 2011. [Online]. Available: https://ar.prysmiangroup.com/Prysmian-secures-SylWin1-project-by-TenneT-for-the-cable-connection-of-offshore-wind-farms-in-the-North-Sea-to-the-German-power-grid. [Accessed: 26-Jan-2019].

[11] "BorWin3 offshore wind project I Projects I Europe I Regions I Petrofac." [Online]. Available: https://www.petrofac.com/en-gb/regions/europe/projects/borwin3-offshore-wind-project/. [Accessed: 27-Oct-2018].

[12] "Tres Amigas : A flexible gateway for renewable energy exchange between the three asynchronous AC networks in the USA," in *Cigre Paris Session*, 2012.

[13] "NordLink - Pioneering VSC-HVDC interconnector between Norway and Germany." [Online]. Available: http://search-ext.abb.com/library/Download.aspx?DocumentID=9AKK106354A2886&LanguageCode=en&DocumentPartId=&Action=Launch. [Accessed: 31-Oct-2018].

[14] D. Van Hertem and M. Ghandhari, "Multi-terminal VSC HVDC for the European supergrid: Obstacles," *Renew. Sustain. Energy Rev.*, vol. 14, no. 9, pp. 3156–3163, 2010.

[15] M. Wang, J. Beerten, and D. Van Hertem, "DC Fault Analysis in Bipolar HVDC Grids."

[16] E. Berne, G. Bergna, P. Egrot, and Q. Wolff, "Earth currents in HVDC grids: An example based on 5 terminal bipolar configurations," in *2014 16th European Conference on Power Electronics and Applications, EPE-ECCE Europe 2014*, 2014.

[17] F. Gonzalez-Longatt, J. L. Rueda, and M. A. M. M. Van Der Meijden, "Effects of grounding configurations on post-contingency performance of MTDC system: A 3-Terminal example," in

Proceedings of the Universities Power Engineering Conference, 2015.

[18] H. Wang, G. Tang, Z. He, and J. Yang, "Efficient grounding for modular multilevel HVDC converters (MMC) on the AC side," *IEEE Trans. Power Deliv.*, vol. 29, no. 3, pp. 1262–1272, 2014.

[19] A. Junyent-Ferre, P. Clemow, M. M. C. Merlin, and T. C. Green, "Operation of HVDC modular multilevel converters under DC pole imbalances," in *2014 16th European Conference on Power Electronics and Applications, EPE-ECCE Europe 2014*, 2014.

[20] M. Wang, W. Leterme, G. Chaffey, J. Beerten, and D. Van Hertem, "Pole Rebalancing Methods for Pole-to-ground Faults in Symmetrical Monopolar HVDC Grids," *IEEE Transactions on Power Delivery*, 2018.

[21] W. Xiang, W. Lin, L. Xu, and J. Wen, "Enhanced Independent Pole Control of Hybrid MMC-HVdc System," *IEEE Trans. Power Deliv.*, vol. 33, no. 2, pp. 861–872, 2018.

[22] M. K. Bucher and C. M. Franck, "Comparison of fault currents in multiterminal HVDC grids with different grounding schemes," in *IEEE Power and Energy Society General Meeting*, 2014.

[23] S. De Boeck, P. Tielens, W. Leterme, and D. Van Hertem, "Configurations and earthing of HVDC grids," *IEEE Power Energy Soc. Gen. Meet.*, pp. 1–5, 2013.

[24] W. Leterme, P. Tielens, S. De Boeck, and D. Van Hertem, "Overview of grounding and configuration options for meshed HVDC grids," *IEEE Trans. Power Deliv.*, vol. 29, no. 6, pp. 2467–2475, 2014.

[25] X. Shi, Z. Wang, B. Liu, Y. Li, L. M. Tolbert, and F. Wang, "Steady-State Modeling of Modular Multilevel Converter under Unbalanced Grid Conditions," *IEEE Trans. Power Electron.*, 2017.

[26] M. Guan and Z. Xu, "Modeling and Control of a Modular Multilevel Converter-Based HVDC System Under Unbalanced Grid Conditions," *IEEE Trans. Power Electron.*, vol. 27, no. 12, pp. 4858–4867, Dec. 2012.

[27] H. Aji, M. Ndreko, M. Popov, and M. A. M. M. van der Meijden, "Investigation on different

negative sequence current control options for MMC-HVDC during single line to ground AC faults," in *2016 IEEE PES Innovative Smart Grid Technologies Conference Europe (ISGT-Europe)*, 2016, pp. 1–6.

[28] A. M. Kulkarni and P. B. Darji, "Dynamic performance of a modular multi-level converter based HVDC terminal under unbalanced AC grid conditions," in *10th IET International Conference on AC and DC Power Transmission (ACDC 2012)*, 2012, pp. 22–22.

[29] G. Falahi and A. Huang, "Control of modular multilevel converter based HVDC systems during asymmetrical grid faults," in *IECON 2014 - 40th Annual Conference of the IEEE Industrial Electronics Society*, 2014, pp. 4595–4600.

[30] Y. Liang, J. Liu, T. Zhang, and Q. Yang, "Arm Current Control Strategy for MMC-HVDC under Unbalanced Conditions," *IEEE Trans. Power Deliv.*, 2017.

[31] G. Li, J. Liang, F. Ma, C. E. Ugalde-Loo, H. Liang, and H. Li, "Analysis of single-phase-to-ground faults at the valve-side of HB-MMCs in bipolar HVDC systems," in *2017 IEEE Energy Conversion Congress and Exposition, ECCE 2017*, 2017.

[32] Y. Yanchen, M. Shicong, and L. Yingbiao, "Analysis and control strategy of unbalanced power in MMC-HVDC grid," *J. Eng.*, vol. 2017, no. 13, pp. 2211–2214, Jan. 2017.

[33] X. Shi, Z. Wang, B. Liu, Y. Liu, L. M. Tolbert, and F. Wang, "Characteristic investigation and control of a modular multilevel converter-based HVDC system under single-line-to-ground fault conditions," *IEEE Trans. Power Electron.*, 2015.

[34] W. H. Weihuang Huang *et al.*, "A calculation method for maximum steady-state loss of VSC-HVDC grounding resistor in Luxi back-back HVDC interconnector," in *12th IET International Conference on AC and DC Power Transmission (ACDC 2016)*, 2016, p. 24 (5 .)-24 (5 .).

[35] M. K. Bucher and C. M. Franck, "Comparison of Fault Currents in Multiterminal HVDC Grids with Different Grounding Schemes," *PES Gen. Meet. | Conf. Expo. 2014 IEEE*, pp. 1–5, 2014.

[36] P. Systems Engineering Committee of the IEEE Industry Applications Society, *IEEE Std 142-*

2007 (Revision of IEEE Std 142-1991) IEEE Recommended Practice for Grounding of Industrial and Commercial Power Systems, vol. 2007. 2007.

[37] S. Liu, Z. Xu, W. Hua, G. Tang, and Y. Xue, "Electromechanical transient modeling of modular multilevel converter based multi-terminal hvdc systems," *IEEE Trans. Power Syst.*, vol. 29, no. 1, pp. 72–83, 2014.

[38] Cigré Working Group B4.57, *Guide for the Development of Models for HVDC Converters in a HVDC Grid*, vol. 604, no. December. 2014.